ANL-77-22

PHYSICS OF REACTOR SAFETY

Quarterly Report

October–December 1976

ARGONNE NATIONAL LABORATORY, ARGONNE, ILLINOIS

Prepared for the U. S. NUCLEAR REGULATORY COMMISSION
Office of Nuclear Regulatory Research

MEMBERS OF ARGONNE UNIVERSITIES ASSOCIATION

The University of Arizona	Kansas State University	The Ohio State University
Carnegie-Mellon University	The University of Kansas	Ohio University
Case Western Reserve University	Loyola University	The Pennsylvania State University
The University of Chicago	Marquette University	Purdue University
University of Cincinnati	Michigan State University	Saint Louis University
Illinois Institute of Technology	The University of Michigan	Southern Illinois University
University of Illinois	University of Minnesota	The University of Texas at Austin
Indiana University	University of Missouri	Washington University
Iowa State University	Northwestern University	Wayne State University
The University of Iowa	University of Notre Dame	The University of Wisconsin

Printed in the United States of America
Available from
National Technical Information Service
U. S. Department of Commerce
5285 Port Royal Road
Springfield, Virginia 22161
Price: Printed Copy $4.00; Microfiche $3.00

Distribution Category:
Advanced Reactor Safety
Research—Fast Reactors
(NRC-7)

ANL-77-22

ARGONNE NATIONAL LABORATORY
9700 South Cass Avenue
Argonne, Illinois 60439

PHYSICS OF REACTOR SAFETY

Quarterly Report
October—December 1976

Applied Physics Division

March 1977

Work performed for the
Division of Reactor Safety Research
U. S. Nuclear Regulatory Commission

Previous reports in this series

ANL-76-13	October—December 1975
ANL-76-72	January—March 1976
ANL-76-114	April—June 1976
ANL-77-9	July—September 1976

TABLE OF CONTENTS

No.		Page
I.	ABSTRACT	1
	TECHNICAL COORDINATION - FAST REACTOR SAFETY ANALYSIS (A2015)	
II.	SUMMARY	1
III.	STUDY OF BASIC PROBLEMS IN ACCIDENT ANALYSIS	2
	A. Initiating Condition Variations	2
	1. Physics Calculations for 2000 Mwe Oxide-Fueled LMFBR	2
	B. Numerical Techniques Used in the PLOOP Code for the Primary Loop Coolant Flow and Heat Transfer Analysis of Certain Pool-Type LMFBR's	2
	C. FX2-POOL Development and Studies	9
	1. Bubble Collapse Autocatalysis in Pools	9
	2. Recriticality	9
	3. Code Development	9
	4. KACHINA Implementation	10
	D. EPIC Development and Studies	10
	1. Code Development	10
	2. EPIC/PLUTO Comparison Studies	10
	3. EPIC Parameter Studies	11
IV.	COORDINATION OF RSR SAFETY RESEARCH	11
	MONTE CARLO ANALYSIS AND CRITICALS PROGRAM PLANNING FOR SAFETY-RELATED CRITICALS (A2018)	
V.	MONTE CARLO ANALYSIS OF SAFETY-RELATED CRITICALS	12
VI.	PLANNING OF DEMO SAFETY RELATED EXPERIMENTS	12
VII.	ANALYTICAL STUDY OF LMFBR OUTLET PLENUM MIXING	14
	REFERENCES	29

LIST OF FIGURES

No.	Title	Page
1.	Variation of Eigenvalue versus Axial Half-Height of the Fuel Slump Region of Phase 4	13
2.	Unit Cell Plate Loading	15
3.	1/15 Scale Model of FFTT Outlet Plenum	17
4.	The Forced Function Used for COMMIX Calculation	18
5.	Velocity Profile Across B-B	20
6.	Velocity Profile Across C-C	21
7.	Velocity Profile Across A-A	22
8.	Velocity Profile Across A-A	23
9.	Velocity Profile Across A-A	24
10.	Velocity Profile Across A-A	25
11.	Temperature Profile at A-A Time = 0.0 Sec	26
12.	Temperature Profile at A-A Time = 10.0 Sec.	26
13.	Temperature Profile at A-A Time = 20.0 Sec.	27
14.	Temperature Profile at A-A Time = 30.0 Sec.	27
15.	A Comparison Between Calculated and Measured Tempuratures At Outlet Nozzle	28

LIST OF TABLES

No.	Title	Page
I.	Reactivity Coefficients for the 2000 MWe (5000 Mwt) High Density Oxide Reactor	3
II.	Eigenvalues of the Various Configurations Proposed for the Experiments	16
III.	Composition of Central Control Rod and Control Rod Position	16
IV.	Worth of a Central Control Rod in the Reference and Fuel-Slump-In Configurations	17

PHYSICS OF REACTOR SAFETY

Quarterly Report
October-December 1976

I. ABSTRACT

This quarterly progress report summarizes work done in Argonne National Laboratory's Applied Physics Division and Components Technology Division for the Division of Reactor Safety Research of the U. S. Nuclear Regulatory Commission during the months of October-December 1976. The work in the Applied Physics Division includes reports on reactor safety research and technical coordination of the RSR safety analysis program by members of the Reactor Safety Appraisals Group Monte Carlo analysis of safety-related critical assembly experiments by members of the Theoretical Fast Reactor Physics Group, and planning of DEMI safety-related critical experiments by members of the Zero Power Reactor (ZPR) Planning and Experiments Group. Work on reactor core thermal-hydraulic performed in the Components Technology Dicision is also included in this report.

TECHNICAL COORDINATION - FAST REACTOR SAFETY ANALYSIS (A2015)

II. SUMMARY

The PLOOP code has been written in a limited effort to study transient coolant flow and heat transfer in the primary loop of pool-type LMFBR's undergoing pump coastdown accidents. Specific features of a primary loop such as motor and pump characteristics and heat exchange are modeled, but pipe rupture is not. The numerical techniques used are explained in detail.

In study of bubble collapse autocatalysis in boiling pools, we have found it important to separate mass, geometry, and leakage effects, since the autocatalysis is caused purely by a leakage effect.

Preliminary results on local overpressurization of boiling pools for 10% of the surface or less indicate very little energy yield, in contrast to the results for uniform overpressurization.

A Distributed Particle-in-Cell routine was incorporated in both POOL and POOLVENS.

Various improvements were made in EPIC, including a pin melt-in model so that fission heating can melt the solid fuel in the pin and increase cavity size during a transient.

Extensive comparison studies have been made between EPIC and PLUTO. Amoung parameters varied in these studies are failure location, cavity temperature and size, and fission gas concentration. Most of the significant differences in the results for the two codes are due to pin numerics, as discussed previously. Further parameter studies with EPIC using features of the code not available in PLUTO are under way.

P. Abramson and H. Hummel, together with W. Sha of ANL and G. Fisher of BNL, visited various laboratories in Europe under NRC sponsorship for the purpose of initiating information exchange on fast reactor safety. The prospects for useful exchange and cooperation seem quite promising.

III. STUDY OF BASIC PROBLEMS IN ACCIDENT ANALYSIS

A. Initiating Condition Variations

1. Physics Calculations for 2000 Mwe Oxide-Fueled LMFBR (P. H. Kier, P. Pizzica and Kalimullah)

Power and reactivity coefficient distributions have been computed for a hypothetical 2000 MWe high density oxide fast breeder reactor. Burnup calculations were run to obtain material compositions for the beginning of an equilibrium cycle. Then r-z, diffusion theory calculations were run to obtain control rod positions that yielded a multiplication constant of near unity, (0.99543) and a fairly uniform power distribution in the core with the reactor at 1100 K and with sodium present. The central control rod was 10 cm above the midplane, the next ring of control rods was fully withdrawn from the core, the next ring of control rods was withdrawn to 7 cm above the midplane and the outer ring of control rods was withdrawn to the midplane of the core. With these control rod positions, real and adjoint flux distributions were computed with the reactor at 1100 K and at 2200 K with sodium both present and voided. Then first order perturbation theory was used to compute sodium worth, steel worth, core fuel worth and Doppler coefficient distributions. These calculations were preformed with the ENDF/B-IV library that was created for the analysis of the Clinch River Breeder Reactor. The results of these perturbation calculations, with the reactivity coefficients aggregated over reactor regions are given in Table I. The core of the reactor was divided into 10 channels and the reactivity coefficient distributions were processed into a form suitable for input to the safety analysis code SAS-3A.

B. Numerical Techniques Used in the PLOOP Code for the Primary Loop Coolant Flow and Heat Transfer Analysis of Certain Pool-Type LMFBR's (Kalimullah)

Because of our prospective close collaboration with the European countries in fast reactor safety research it seems to be worthwhile to acquire a better understanding of the characteristics of pool-type LMFBR's, even if such reactors do not become of interest in the U.S. Recent pool reactor studies at ANL, although quite limited, afforded us an occasion to become involved in study of pool reactors to some extent. A small (ca. 3 man-month) effort has been undertaken to write a code for analyzing transient coolant flow and heat transfer in the primary loop of pool-type LMFBR's. In its initial version now completed, the code is limited to dealing with cold pool reactors not containing any free sodium surface in the reactor outlet plenum (as typified by

TABLE I. Reactivity Coefficients for the 2000 MWe (5000 Mwt) High Density Oxide Reactor

Type	Fluxes	Inner Core	Outer Core	Lower Axial Blanket	Upper Axial Blanket	Radial Blanket	Total
Power (MW)	1100K, Na in	1204.44	708.62	26.28	15.53	45.19	2000
Sodium Void ($\Delta k/k \times 10^3$)	1100K, Na in	14.63	3.63	-0.06	-0.08	-0.11	18.01
	1100K, Na out	17.84	4.20	0.24	0.03	0.11	22.43
Steel Worth ($\Delta k/k \times 10^3$)	1100K, Na in	-58.34	-16.96	1.09	0.70	1.19	-72.32
	2200K, Na in	-59.67	-17.93	1.05	0.68	1.18	-74.69
	1100K, Na out	-62.60	-15.61	1.47	0.99	1.39	-74.36
	2200K, Na out	-64.15	-16.39	1.40	0.96	1.35	-76.83
Doppler 1100-2200K $-\frac{1}{k}\frac{dk}{dt} \times 10^4$	1100K, Na in	75.41	26.23	3.56	1.13	2.99	109.34
	1100K, Na out	58.76	18.13	3.35	1.12	2.59	83.96
Doppler 2200-4400K $-\frac{1}{k}\frac{dk}{dt} \times 10^4$	2200K, Na in	66.58	23.69	3.08	0.99	2.60	96.95
	2200K, Na out	51,23	16.09	2.84	0.95	2.20	73.32
Core Fuel Worth ($\Delta k/k \times 10^3$)	1100K, Na in	202.45	123.09	15.26	6.04		346.84
	2200K, Na in	205.15	127.72	14.87	5.99		353.73
	1100K, Na out	217.81	117.61	17.57	7.56		360.55
	2200K, Na out	220.07	120.75	17.21	7.52		365.55

EBR-II) and with piping intact (i.e., pipe rupture accidents are not modeled). Modified cold pool reactors of this type were of interest in the ANL studies because they eliminate or at least mitigate some of the undesirable features of both the hot pool (as typified generally by the French PHENIX and the British PFR with the undesirable features of the shield deck and the main tank facing hot sodium) and the cold pool (as typified generally by EBR-II with the undersirable feature of thermal transients at the reactor outlet) while retaining most of the advantages of both. However, PLOOP can easily be extended to study hot pool reactors if desired.

The capabilities of the PLOOP code include explicit accounting of the electric motor and the primary pump characteristics, heat exchange with the intermediate loop, heat exchange of all components with the main tank sodium, natural circulation, start-up transient, generation of full power conditions and flow coastdown transient. Although the code computes the spatial and temporal variations of mass flow rate and temperature of the coolant on the tube side(the intermediate loop side) of the IHX, the values of these quantities at the inlet to the tubes are input constants. It is not currently planned to incorporate PLOOP into SAS as our present objectives for studies with PLOOP do not require.

With a view to summarize here the overall structure of the code, the basic numerical technique used for advancing the time is outlined leaving out the details of the geometry of the system. The thermodynamic properties of liquid soidium are assumed to depend only on its temperature and not on its pressure. Since flow work is negligible compared to heat transfer, the specific enthalpy of the coolant is assumed equal to the specific internal energy. Pressure waves have been eliminated from the code by using only one integral momentum equation between any pair of free surfaces (or around a closed circuit if there is not any free surface) to determine flow rate.

Since there is no free sodium surface in the reactor outlet plenum, the primary loop of the geometrically intact reactor system consists of only one closed circuit of flow, everywhere full of sodium, and this makes it possible to determine the temporal variation of mass flow rate with the help of only one integral momentum equation for the whole circuit. For heat transport calculations this flow circuit is divided into N_h small nearly equal volumes (heat transfer nodes). Use of nearly equal volumes with a time step less than but as close as possible to $\rho\Delta V/W$ (where ρ is density, ΔV node volume and W mass flow rate) is expected to cause less numerical diffusion of energy along the flow path. Some nodes can be used to represent large well-mixed volumes, i.e., the main tank, inlet plenum, outlet plenum, etc. by option. Other components in the loop are represented by one or more heat transfer nodes. The main tank constitutes node 1 and the node at the IHX exit is the last.

The main quantities whose temporal variation is determined from differential equations are (the superscript n denotes time t^n)

U_j^n , $j = 1,2, \ldots N_h$ = Internal energy of node j,

W_j^n , j = 1,2, . . . $(N_h + 1)$ = Mass flow rate at the inlet boundary of node j,

ω^n = Pump-motor angular speed,

M_1^n = Mass of sodium in the main tank (node 1),

UI_j^n = Internal energy of node j on the tube side (intermediate loop side) of the IHX,

and WI_j^n = Mass flow rate at the inlet boundary of node j on the tube side of the IHX.

The subsidiary quantities whose temporal variation is computed from the above main quantities with the help of algebraic relations, i.e., sodium properties, pump characterisitics, motor characteristics, etc., include the primary loop nodal temperature T_j^n, nodal density ρ_j^n, nodal specific enthalpy H_j^n, the intermediate loop nodal tempurature TI_j^n, nodal specific enthalpy HI_j^n, torque developed by the motor τ_m^n, hydraulic torque required by the pump τ_p^n, head developed by the pump ΔH^n and others.

The following steps of computation are followed in advancing to time t^{n+1} from time t^n.

Step 1: The differential equation of energy conservation for the heat transfer node j can be written as

$$\frac{dU_j}{dt} = (W_j, W_{j+1}, H_{j-1}, H_j, H_{j+1})_{donor} + Q_j, \quad j = 1,2,\ldots N_h, \qquad (1)$$

where the parenthetical term implies the rate of heat energy undergoing advection into the node j computed using the donor cell concept, and Q_j is the rate of heat transfer into the node through its walls from the surrounding fluid, i.e., the main tank sodium (and the inert gas atmosphere around the outer surface of the main tank in the case of node 1). Using Eq. (1) U_j^{n+1} is computed.

$$U_j^{n+1} = U_j^n + \Delta t \left[Q_j^n + (W_j, W_{j+1}, H_{j-1}, H_j, H_{j+1})_{donor}^n \right] , \quad j = 1,2,\ldots N_h . \quad (2)$$

Step 2: Using the integral momentum equation described below, the mass flow rate at inlet to the pump from the main tank at time t^{n+1}, that is, W_2^{n+1} is computed.

Step 3: The code stores liquid sodium temperature as a function of the product of density and specific enthalpy, and density as a function of temperature

$$T = TEMP(\rho H), \quad (3)$$

and $$\rho = RHOL(T). \quad (4)$$

Using Eqs. (3) and (4) the nodal temperatures, densities and specific enthalpies at time t^{n+1} are evaluated (except node 1, the main tank).

$$T_j^{n+1} = TEMP \left(U_j^{n+1} \Big/ \Delta V_j \right), \quad j = 2,3,\ldots N_h , \quad (5)$$

$$\rho_j^{n+1} = RHOL \left(T_j^{n+1} \right) , \quad j = 2,3,\ldots N_h \quad (6)$$

and $$H_j^{n+1} = U_j^{n+1} \Big/ \left(\rho_j^{n+1} \ \Delta V_j \right) , \quad j = 2,3,\ldots N_h . \quad (7)$$

Step 4: Since the volume of the coolant in the main tank does not remain constant, Step 3 can not be applied to compute main tank sodium temperature, density and specific enthalpy. The differential equation for the mass of sodium in the main tank can be written as

$$\frac{dM_1}{dt} = N_x W_{N_h+1} - N_p W_2 , \quad (8)$$

where N_p and N_x are the numbers of pumps and IHXs respectively in the primary loop system. Using Eq. (8) M_1^{n+1} is computed, and then from U_1^{n+1} and M_1^{n+1} and the stored liquid sodium temperature as a function of its specific enthalpy,

$$T = TEMPH(H), \quad (9)$$

the specific enthalpy, temperature and density of node 1 are computed.

$$M_1^{n+1} = M_1^n + \Delta t \left(N_x W_{N_h+1}^n - N_p W_2^n \right), \tag{10}$$

$$H_1^{n+1} = U_1^{n+1} \Big/ M_1^{n+1}, \tag{11}$$

$$T_1^{n+1} = \text{TEMPH} \left(H_1^{n+1} \right), \tag{12}$$

$$\rho_1^{n+1} = \text{RHOL} \left(T_1^{n+1} \right). \tag{13}$$

Step 5: The differential equation of mass conservation for the heat transfer node j (except node 1, the main tank) can be written as

$$C_T \frac{dU_j}{dt} = W_{j+1} - W_j, \tag{14}$$

where $C_T(T) = -\frac{d\rho}{d(\rho H)}$ and is stored for liquid sodium as a function of temperature. Starting from W_2^{n+1} computed in Step 2, the mass flow rates at other node boundaries (except W_1 which is not a relevant quantity) are computed recursively.

$$W_{j+1}^{n+1} = W_j^{n+1} + C_T \left(\frac{T_j^n + T_j^{n+1}}{2} \right) \frac{U_j^{n+1} - U_j^n}{\Delta t}, \quad j = 2,3,\ldots N_h. \tag{15}$$

Step 6: The techniques used in computing the tube side variables at time t^{n+1} i.e., UI_j^{n+1}, WI_j^{n+1}, TI_j^{n+1} and HI_j^{n+1} are the same as those used on the primary side except that the mass flow rate at the tube side inlet is not computed using an integral momentum equation but is an input to the code. Furthermore, the tube side sodium density is never computed because it is not required.

In the first cycle of calculations to advance from time t^n to t^{n+1}, almost all time-derivatives (i.e., Steps 1, 2 and 4) are evaluated at the beginning of the time step. In the second and higher cycles of calculations over the same time step, the average of the values of all the time-dependent variables at the times t^n and t^{n+1} are used in evaluating the derivatives. Any number of cycles over a time step may be specified in the code.

The Integral Momentum Equation: The differential equation of momentum conservation for the component ι (which is represented by one or more heat transfer nodes) can be written as (except the component representing the pump)

$$I_\iota R_\iota A_{x,\iota} \frac{dW_2}{dt} = p_{in,\iota} - p_{ex,\iota} + \bar{\rho}_\iota g\left(Z_{in,\iota} - Z_{ex,\iota}\right)$$

$$+\Delta p_{mom,\iota} - \Delta p_{maj,\iota} - \Delta p_{min,\iota} \quad , \quad \iota = 1,2,\ldots N_c, \tag{16}$$

where p is pressure, Z elevation above an arbitrary reference, the subscripts in and ex represent inlet and exit to the component, $\bar{\rho}_\iota$ is the average density of the component ι, $\Delta p_{mom,\iota}$ the momentum flux term, $\Delta p_{maj,\iota}$ and $\Delta p_{min,\iota}$ are the major and minor frictional pressure drops, I_ι is the geometric inertia, $A_{x,\iota}$ the number of (identical) pumps causing mass flow into (each identical) component ι, and R_ι is the flow ratio defined as

$$R_\iota = (\text{Mass flow rate through component } \iota \text{ averaged over its flow path length}) \,/\, (A_{x,\iota}\, W_2) \,. \tag{17}$$

The left side of the momentum equation for the component representing the pump contains an additional term $\bar{\rho}_p g\Delta H(\omega, R_p W_2/\bar{\rho}_p)$ for the pump head (where the subscript p refers to the pump.) Summing the momentum equations of all the N_c components, the pressures cancel out and the following equation for the whole loop is obtained:

$$\sum_{\iota=1}^{N_c} I_\iota R_\iota A_{x,\iota} \frac{dW_2}{dt} = \sum_{\iota=1}^{N_c}\left[\bar{\rho}_\iota g\left(Z_{in,\iota} - Z_{ex,\iota}\right) + \Delta p_{mom,\iota} - \Delta p_{maj,\iota}\right.$$

$$\left. - \Delta p_{min,\iota}\right] + \bar{\rho}_p g\Delta H \left(\omega, R_p W_2/\bar{\rho}_p\right) \,. \tag{18}$$

Since the calculation of the pump head involves the pump-motor angular speed, the following differential equation for the angular speed is also solved:

$$I_{pm} \frac{d\omega}{dt} = \tau_m(E, \omega) - \tau_p\left(\omega, R_p W_2/\bar{\rho}_p\right) \frac{\bar{\rho}_p}{\rho_{pr}} - \tau_{fr} \frac{\omega|\omega|}{\omega_r^2} \quad , \tag{19}$$

where I_{pm} is pump-motor moment of inertia; $\tau_m(E,\omega)$ is the torque developed by

the electric motor at the applied voltage E and angular speed ω; $\tau_p(\omega, R_p W_2/\bar{\rho}_p)$ is the hydraulic torque required by the pump at the angular speed ω and volumetric flow rate $R_p W_2/\bar{\rho}_p$; τ_{fr} is the rated mechanical frictional torque on the pump-motor shaft at the rated angular speed ω_r.

In the first cycle of calculations to advance from time t^n to t^{n+1}, the values of the pump inlet mass flow rate and the pump-motor angular speed at the end of the time step are computed using Eqs. (18) and (19) as follows:

$$W_2^{n+1} = W_2^n + \Delta t \left(\frac{dW_2}{dt}\right)^n , \tag{20}$$

and $$\omega^{n+1} = \omega^n + \Delta t \left(\frac{d\omega}{dt}\right)^n . \tag{21}$$

C. FX2-POOL Development and Studies

1. Bubble Collapse Autocatalysis in Pools (T. Daly and P. Abramson)

We have found that the initial conditions in pools can make very significant differences in the energetics of a prompt critical burst for a pool subjected to a specific physical perturbation. In particular, a homogeneous pool that is prompt critical will not represent a prompt critical situation when the same mass is redistributed in the same volume at the same average cell densities into full density liquid and bubbles, but will be several dollars subcritical. Thus to study the autocatalysis of bubble collapse, one must be cautious to separate mass, geometry and leakage effects-since the autocatalysis we are interested in is purely a leakage effect.

2. Recriticality (T. Daly and P. Abramson)

A new explicit technique for coupling the neutronics and hydrodynamics portions of FX2-POOL was written and checked out and initial results are available for boiling pools subjected to local over pressures. Preliminary results indicate that while significant energy can be deposited due to a uniform over pressurization, a local pressurization of less than 10% of the surface (in R/Z Geometry) appears to yield very little energy.

3. Code Development (P. Abramson)

A generalized Distributed-Particle-In-Cell routine was incorporated in both POOL and POOLVENS and was included in the versions shipped to GfK as well as those being used for recriticality and autocatalysis problems.

A color movie was made in which the temperature of the fuel was used to determine the color of the particles. This movie demonstrates the importance of fuel to steel heat transfer following a prompt burst and follows motions out until the core two-phase bubble essentially occupies all of the original active core volume.

4. KACHINA Implementation (J. J. Sienicki)

KACHINA was adopted to the ANL 370-195, a sample problem was obtained from J. Travis of LASL and was successfully run with our version.

D. EPIC Development and Studies

1. Code Development (P. Pizzica)

The following improvements were made in EPIC. A plotting program was completed which will display results from EPIC/PLUTO comparison studies and from the EPIC parameter study. A particle combination routine was added so that particles in the channel could be reduced. A variation of the limits on the number of particles in the channel showed how much the number of particles could be reduced without distorting the results over the uncombined case. This reduced the new time by a factor of 2. A pin melt-in model was added so that fission heating can melt the solid fuel in the pin and increase the cavity size. Condicution effects are neglected. The momentum equations for both the pin and the channel were made fully implicit in time while the rest of the code is still semi-implicit. This eliminated numerical instabilities that occasionally resulted from the convective flux terms when the equations were no longer pressure-driven far out in the transient. This allowed a larger time step with no change in the results.

2. EPIC/PLUTO Comparison Studies (P. Pizzica and J. Sienicki)

Much effort was expended on the EPIC/PLUTO comparison studies. The reactor initial conditions for most of the cases correspond to TOP conditions. However, LOF-TOP conditions are used in a number of cases where the two codes can reasonably be compared. Different void fractions and inlet plenum pressures are used. The basic geometry used for the comparison is that of a demonstration size reactor, and the following parameters characteristics are varied.

- Four different failure locations are compared (using a 5 cm long single node failure because of PLUTO's limitation): one 15 cm below the core center, at the center, 15 cm above and 30 cm above.

- Three different initial pin cavity homogenized temperatures are used: 3500°K, 4000°K and 4500°K.

- EPIC uses an axially varying temperature in another case whose average corresponded to the 3500°K PLUTO case.

- Three different levels of fission gas concentrations are compared for the two codes.

- Different amounts of void (determining the cavity pressure in the ideal fission gas partial pressure calculation) are used.

- The melt fraction of the cavity is 25%, 50%, 75% and 100% at the failure (the shape of the cavity was assumed to be a rotational ellipsoid).

- EPIC's slip calculation between fission gas and fuel in the cavity is compared to PLUTO's homogeneous calculation.

- EPIC's fission heating and melt-in are compared to PLUTO's case without these features.

Preliminary results indicate that EPIC and PLUTO give reasonable agreement over differences up to roughly 100% in significant parameters. Most of the significant differences seen are due to the difference in pin numerics, which was thoroughly discussed in the January-March 1976 Quarterly.

3. EPIC Parameter Studies (P. Pizzica and J. Sienicki)

Some preliminary calculation were done for the EPIC parameter study on which work will begin in the very near future. Parameters to be varied include pin failure location, failure length (and expansion of rip with time), initial void fraction in the collant channel (uniform voiding in front of the rip and discontinuous voiding patterns simulating bubbles), initial fuel temperature, heating rate (including studies of solid fuel melt-in in the pin cavity), fission gas content and void volume in the pin cavity, initial sodium flow rate and pump head, slip between fission gas and fuel in the pin cavity or no slip and the melt fraction of the fuel pin. The calculations which have been done are for LOF-TOP conditions where the channel was 60% uniformly voided in front of the failure for half the core height for 3500°K and if 500°K initial fuel temperatures two different fission gas concentrations, single and four-node failures, also the 3500°K case was done with an 80% voided channel and an unvoided channel and a four-node failure into an unvoided channel. Results are still preliminary (when all work is completed it will be reported).

IV. COORDINATION OF RSR SAFETY RESEARCH

P. Abramson and H. Hummel were members of an NRC-sponsored team that visited European nuclear energy laboratories in November 1976, with a view to initiate information exchange on fast reactor safety. Other team members were W. Sha, Components Technology Division, ANL, and G. Fischer of Brookhaven, currently on assignment to CEA, Saclay. Visits were made to Risley, Culcheth, and Winfrith in England, GfK, Karlsruhe, Germany, the Euratom Joint Research Center, Ispra, Italy, and to Cadarache, Saclay, and Grenoble in France. We found everywhere a great interest in cooperative effort and information exchange in fast reactor safety, and regard the prospects for such cooperation as very bright. We did not find much in the way of code development that appeared to be immediately useful to us except for the British SABRE thermohydraulics code, although the scale of effort is such that there should certainly be analytical developments useful to us in the future. Of greatest immediate interest to us aside from the SABRE code is the experimental work in thermohydraulics, in FCI, in fission-gas dispersal of fuel (VIPER experiments), in PAHR, and in explosion containment. The DFR loss-of-flow experiments are of particular interest. The CABRI (TOP) and SCARABEE (LOF) experiments to be conducted at Cadarche will be of great interest. First results from CABRI are expected later this year.

During the visit in Europe we discussed the possiblity of our participation in the work of the European WAC (Whole Core Accident) Committee.

Arrangements for this are now being made. A current project of this committee is the comparison of accident calculations for a model of a 1000 Mwe LMFBR.

Per agreements at GfK (Karlsruhe), Abramson sent a complete tape of all POOL subroutines to Peter Royl and Hans Buchner at GfK so they can begin their portion of our co-operative development effort (which is to develop a more sophisticated treatment of boundary heat transfer and to generalize the routines).

Also, per those agreements, J. Sienicki sent a sample problem we ran with our IBM version of KACHINA to Philip Schmuck at Karlsruhe and we are awaiting receipt of his sample problems for us to run.

P. Pizzica attended a tutorial on SIMMER at LASL, November 3-5, 1976.

P. Abramson attended a 2 day meeting on LOF-TOP and on FCI's on December 9-10, as a consultant to NRC DPM, and visited BNL on December 17 for discussions on SIMMER validation with C. Durston and O. Jones.

MONTE CARLO ANALYSIS AND CRITICALS PROGRAM PLANNING FOR SAFETY-RELATED CRITICALS (A2018)

V. MONTE CARLO ANALYSIS OF SAFETY-RELATED CRITICALS

Monte Carlo calculations for the R-Z homogeneous model of the Step 5 core have now been com pleted. We find that VIM gives $\lambda = 1.013 \pm 0.002$, while the diffusion theory eigenvalue is 1.000. S_n calculations for the same core will be run next but it is not clear, at this point, whether these computations should be run on DOT or TWOTRAN. A small discrepancy between DOT and TWOTRAN eigenvalues has been noted during this last report period, and this discrepancy is now under investigation. As reported earlier the TWOTRAN S_4-P_1 eigervalue for step 1 is 1.0093. The DOT eigenvalue, for the same space mesh and angular quadrature set, is 1.0078. Though the discrepancy is small it's cause is unknown and it is, therefore disturbing. DOT and TWOTRAN k_∞ calculations, for the step 1 core material, are now being run for diagnostic purposes, and other sorts of consistency checks will also be run.

VI. PLANNING OF DEMO SAFETY RELATED EXPERIMENTS

This quarterly report presents results of additional preanalysis performed to help in the planning of the safety related critical experiments. The calculations focused on four areas, viz:

a. Adjustment of system reactivity by varying the axial extent of the fuel slump region.

b. Reactivity of a partial fuel slump-in configuration.

c. Reactivity of the fuel slump-out configuration.

d. Reactivity worth of a central control rod in Phases I (reference) and IV (fuel slump-in) configuration (see previous quarterly report).

The analyses of items a and d were suggested by the Fast Reactor Critical Experiment Review Group[1] in October 1976. Items b and c were studied as part of the ongoing preanalysis program. Results of the calculations will be described in some detail in the following paragraphs.

The adjustment of the system reactivity by varying the axial extent of the fuel-slump region (and thereby not conserving fuel in the assembly) has been studied to determine the potential of this method. The fuel-slump region in Phase IV occupies the central 37 drawers ($r \leq 18.96$ cm) and contains "double-density" fuel.[1] If this central core region slumps to one-half its original height (i.e., to an axial half-height of 23.09 cm), the eigenvalue is 1.0503. The variation of eigenvalue versus axial extent of the fuel slump region has been calculated and is presented in Fig. 1. The critical value for this dimension is 17.30 (or 6.81 in.) in each assembly half. This corresponds to a critical mass of 212.2 kg (including 46.6 kg in the fuel-slump region). The above configuration could be obtained by loading a 7-in. fuel-slump region in each assembly half which would require only a small additional adjustment to critical. These preliminary results indicate such an adjustment of the system reactivity is feasible.

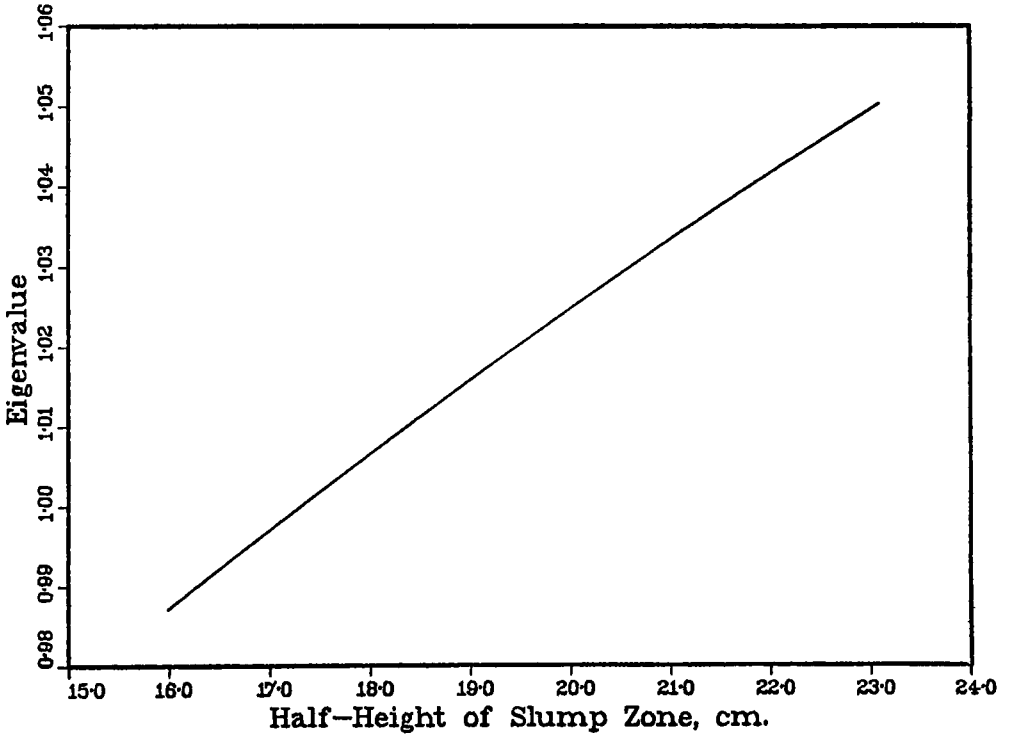

Fig. 1. Variation of Eigenvalue versus Axial Half-Height of the Fuel Slump Region of Phase 4
ANL Neg. No. 116-77-209

An intermediate fuel slump-in configuration was designed for the calculation of the reactivity of a partial fuel slump-in condition. In the reference core unit cell there are two 1/4-in. fuel columns (1/2-in. fuel, 1/2-in. Fe_2O_3 with all sodium removed). For the intermediate fuel slump-in configuration, the damaged region occupies the central 37 drawers of the assembly with a three-fuel-column unit cell composition in the outer axial core region (23.09 cm < H $\leq$ 46.18 cm). These unit cells are shown in Fig. 2. The eigenvalue for this partial fuel slump configuration was 1.0352. This value is intermediate to the k_{eff} 0.9993 for the Phase II configuration (sodium voided in central 37 drawer zone) and the k_{eff} of 1.0503 for the Phase IV configuration (total fuel slump in the central 37 drawer zone).

Eigenvalue calculations were performed for the two "fuel slump-out" configurations.[1] In the Phase III, Step A configuration the double-density fuel slump ($r \leq 18.96$ cm, which corresponds to the central 37 drawers) is shifted to the outer axial portions ($23.09 < |Z| \leq 46.18$ cm) of the core. In Phase III, Step B this fuel slump is shifted out to the axial blankets ($46.18 \text{ cm} < |Z| \leq 69.27$ cm). The eigenvalues are 0.9864 and 0.9065 respectively. Eigenvalues computed for all phases or configurations of the proposed experimental plan are listed in Table II. The large subcriticalities involved in these configurations, particularly for Phase III, Step B will necessitate careful attention to the experimental methods used in these configurations to ensure their validity.

The worth of a central control rod in the reference (Phase I) and "fuel slump-in" (Phase IV) configurations was calculated. The control rod position occupied the central 4 drawers ($r \leq 6.2337$ cm) and extended the entire length of the assembly. The inserted rod extended the length of the normal core. Number densities for the control rod and control rod position are given in Table III. The eigenvalues for the various configurations are summarized in Table IV. The 4-drawer control rod used in these calculations represents a typical LMFBR control rod and as such is large for this smaller assembly. Because of this a smaller (single drawer) control rod might be considered for the actual measurements.

VI. ANALYTICAL STUDY OF LMFBR OUTLET PLENUM MIXING

Accurate predictions of in-reactor-vessel thermal hydraulic characteristics such as flow pattern, degree of mixing, flow distribution, pressure drop, coolant velocities, flow induced vibration, thermal striping, buoyancy effects and stratification are essential to improve reactor performance and to prevent the occurrence of an abnormality which might lead to a reactor accident situation. The present study is specifically directed toward investigating the thermal hydraulic behavior of the liquid metal fast breeder reactor (LMFBR) outlet plenums during reactor scram conditions.

Under normal reactor operating conditions, sodium enters the outlet plenum of an LMFBR via an inlet structure, and after mixing within the plenum, exits through three outlet nozzles as shown in Fig. 3. During a reactor scram transient, the plenum experiences an abrupt decreasing of the entering sodium temperature and correspondingly an increasing of the entering sodium density. If the entering lower temperature sodium has sufficient inertial force to counter balance the opposite buoyancy force, a high degree of

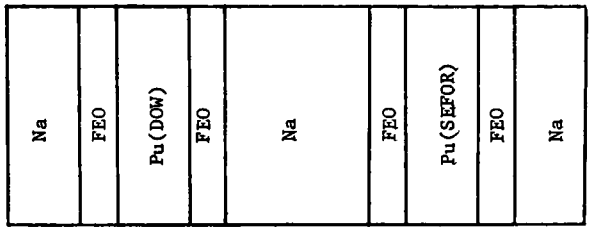

REFERENCE CORE UNIT CELL
(2 FUEL COLUMNS)

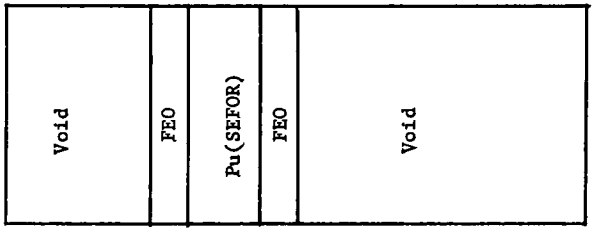

PARTIAL FUEL SLUMP UNIT CELL
(1 FUEL COLUMN)

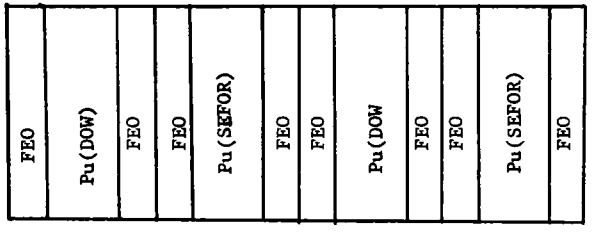

SLUMPED FUEL UNIT CELL
(4 FUEL COLUMNS)

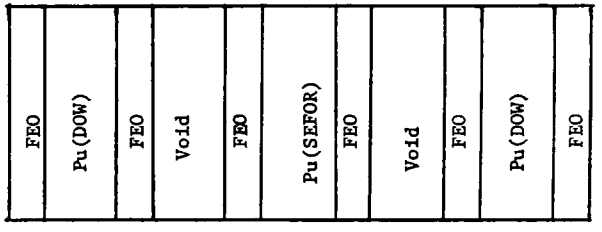

PARTIAL FUEL SLUMP UNIT CELL
(3 FUEL COLUMNS)

KEY:

UO = U_3O_8 Plate

Na = Na Can

FEO = Fe_2O_3 Plate

Pu (DOW) = Pu/U/Mo CAN (0.282/0.691/0.025, $^{239}Pu/Pu = 0.907$)

Pu (SEFOR) = Pu/U/Mo CAN (0.195/0.779/0.026, $^{239}Pu/Pu = 0.870$)

Fig. 2. Unit Cell Plate Loading
ANL Neg. No. 116-77-200

TABLE II. Eigenvalues of the Various Configurations Proposed for the Experiments

Phase 1, Reference Configuration R_{Core} = 46.18 cm $R_{Blanket}$ = 86.18 cm H/D = 1.0	k = 1.0000
Phase 2, Void Na for $r \leq 18.96$ cm, $Z \leq 86.18$ cm	k = 0.9993
Phase 3, Step A Fuel Slump Out $r \leq 18.96$ cm, 23.09 cm $\leq \|Z\| \leq$ 46.18 cm	k = 0.9864
Phase 3, Step B Fuel Slump Out $r \leq 18.96$ cm, 46.18 cm $\leq \|Z\| \leq$ 69.27 cm	k = 0.9065
Phase 4, Fuel Slump In $r \leq 18.96$ cm, $Z \leq 23.09$ cm	k = 1.0503
Phase 4, Fuel Slump In $r \leq 18.96$ cm, $Z \leq 17.30$ cm	k = 1.0000
Phase 5, Fuel and Blanket Slumped in, $r \leq 18.96$ cm, $Z_{fuel} \leq 17.30$ cm $Z_{Blanket} \leq 57.30$ cm	k = 1.0201

TABLE III. Composition of Central Control Rod and Control Rod Position

	Number Density, 10^{24} atoms/cm^3			
Isotope	Sodium Filled CRP	Sodium Voided CRP	Na-Filled Control Rod	Na-Voided Control Rod
^{10}B	-	-	0.012189	0.012189
^{11}B	-	-	0.049427	0.049427
Na	0.018606	0 -	0.003959	-
Fe	0.010684	0.010684	0.009277	0.009277
Ni	0.001385	0.001385	0.001159	0.001159
Cr	0.003015	0.003015	0.002558	0.002558
Mn	0.000250	0.000250	0.000217	0.000217
Mo	0.000022	0.000022	0.000021	0.000021
O	0.000038	0.000038	0.015891	0.015891

TABLE IV. Worth of a Central Control Rod in the Reference and Fuel-Slump-In Configurations

		Eigenvalue	$\frac{k_{ROD} - k_{CRP}}{k_{CRP}}$
Phase I	Reference Configuration	1.0000	
Phase I	With Na-Filled Control Rod Position	0.9823	-0.0532
Phase I	With Control Rod	0.9300	
Phase IV	Fuel Slump In	1.000	
Phase IV	With Na-Filled Control Rod Position	0.9762	-0.0488
Phase IV	With Na-Filled Control Rod	0.9286	
Phase IV	With Na-Voided Control Rod Position	0.9698	-0.0433
Phase IV	With Na-Voided Control Rod	0.9278	

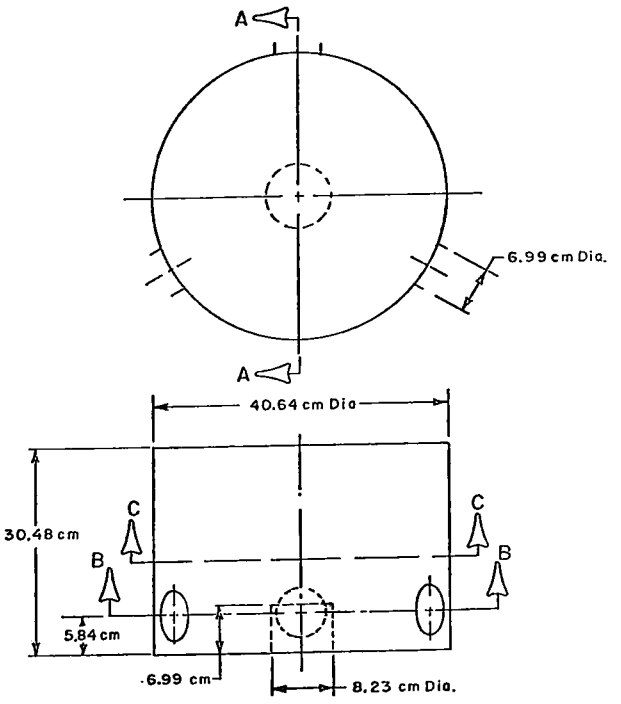

Fig. 3 1/15 Scale Model of FFTT Outlet Plenum
ANL Neg. No. 116-77-210

mixing is ensured. On the other hand, if the entering colder sodium has insufficient inertial force to overcome the opposite bouyancy force, a potential exists for severe thermal shock to plenum components, especially the outlet nozzles. Furthermore, a stratified flow pattern could exist, having a sharp thermal discontinuity within the plenum and might introduce intolerable thermal stress of the affected components.

In recent years, numerical simulation of thermal hydraulic problems has made striking advances [1,10], and its increasing importance in solving engineering problems is anticipated for many years to come. Up to this date, however, the numberical simulation of the LMFBR outlet plenum is limited to one [11] and two dimensions [12,13,14]. As shown in Fig. 3, the outlet nozzles are located 120° apart, and in general the various components and supporting structures located in the outlet plenum region are non-symmetric, thus, both the temperature and velocity fields of the outlet plenum have inherent three dimensional characteristics. In order to carry out a realistic evaluation of the outlet plenum mixing, a three dimensional analysis is necessary.

In this study, the newly developed COMMIX (Component Mixing) computer program [15] is used. The COMMIX is a three-dimensional, transient, two-phase flow with non-equilibrium temperatures and velocities, thermal hydraulic analysis code in which the two fluid model based on multidomain multi-phase fluid mechanics [16] and the IMF (implicit multifield) numerical scheme are employed [10]. This development work is visualized to be in stages, with improving rigor and accuracy as well as enlarging the scope of applications. At the present time, only the single-phase with xyz cartesian coordinates version is working. Modification of xyz cartesian coordinates to treat curved boundary are in progress [17].

Two cases of outlet plenum mixing [18], which are of practical interest, have been investigated thoroughly. One is the constant flow scram in which the density of the entering sodium is suddenly increased while the inlet flowrate is maintained constant. The other case is the normal scram in which the density change is accompanied by a flow coast down to 10% of the initial flowrate. Fig. 4 presents the forced function used in the COMMIX transient

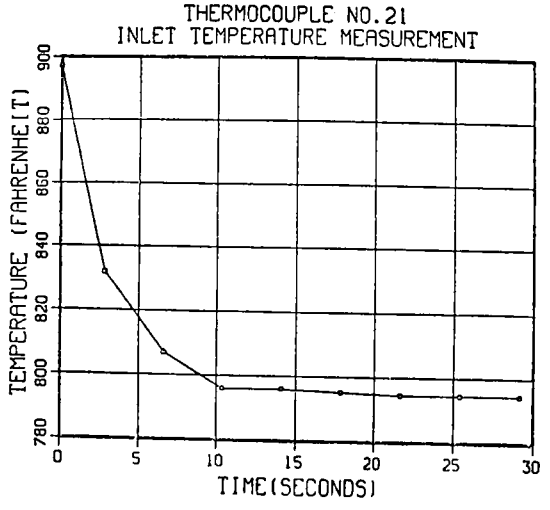

Fig. 4
The Forced Function Used for COMMIX Calculation. ANL Neg. No. 116-77-211

calculation fo instant flows scram. Figs. 5 and 6 present the velocity profiles at the steady state along sections B-B and C-C as shown in Fig. 3, respectively. Both velocity and temperature profiles across section A-A are shown in Figs. 7-10 and Figs. 11-14 respectively. The experimentally measured coolant temperatures [18] at the exit nozzle and the predicted temperatures by the COMMIX code during the transient are shown in Fig. 15. The agreements between the measured and predicted results are good.

Based on this study, it is concluded that the numerical simulations presented here provide a reasonable confidence in design of the outlet plenum, and further study of transients under the wide range of reactor operating conditions will lead to improved plenum design. Thus the potentially hazardous thermal shocks can be identified and avoided, and the structural integrity of the affected reactor components can be maintained.

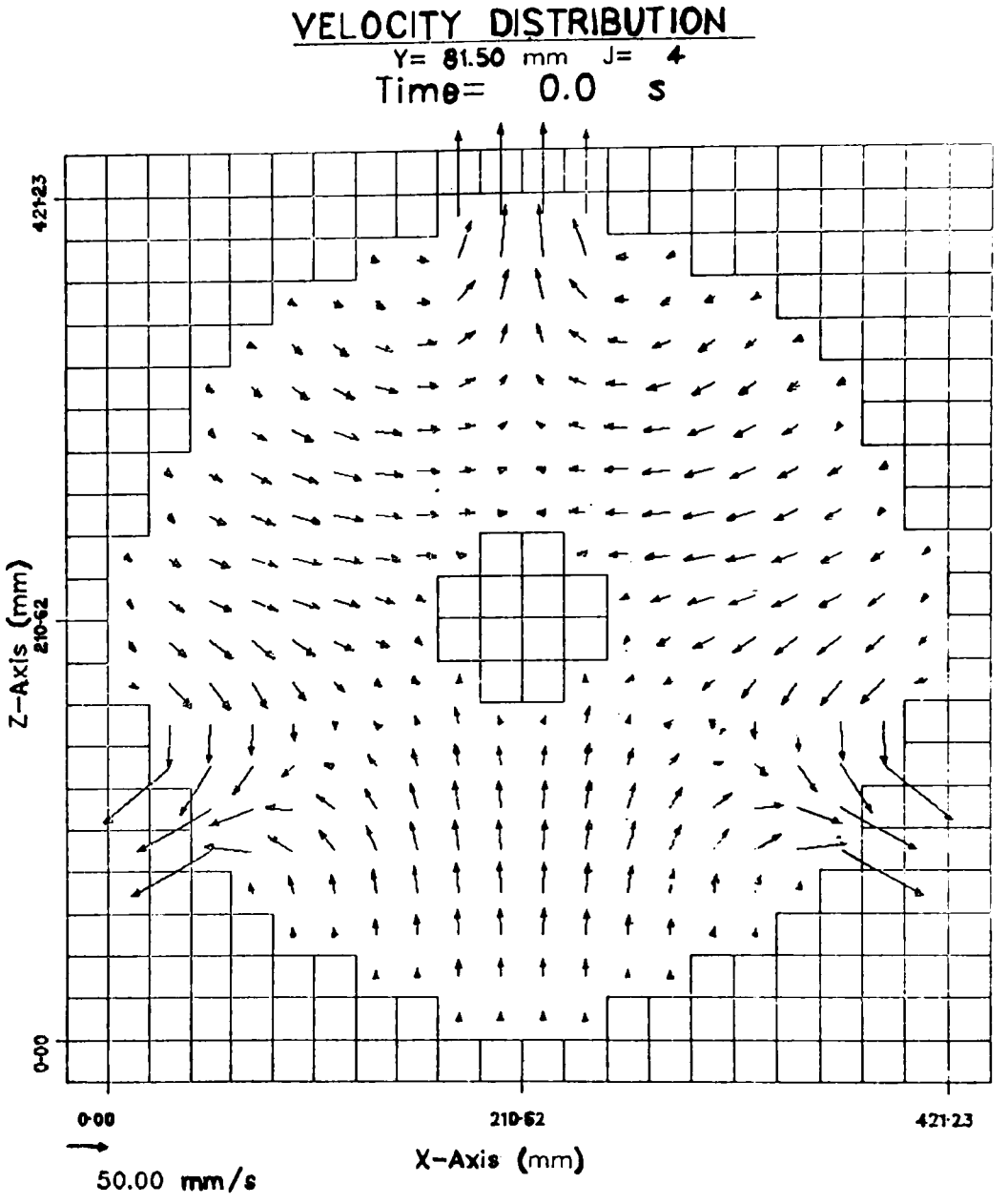

Fig. 5. Velocity Profile Across B-B
ANL Neg. No. 116-77-208

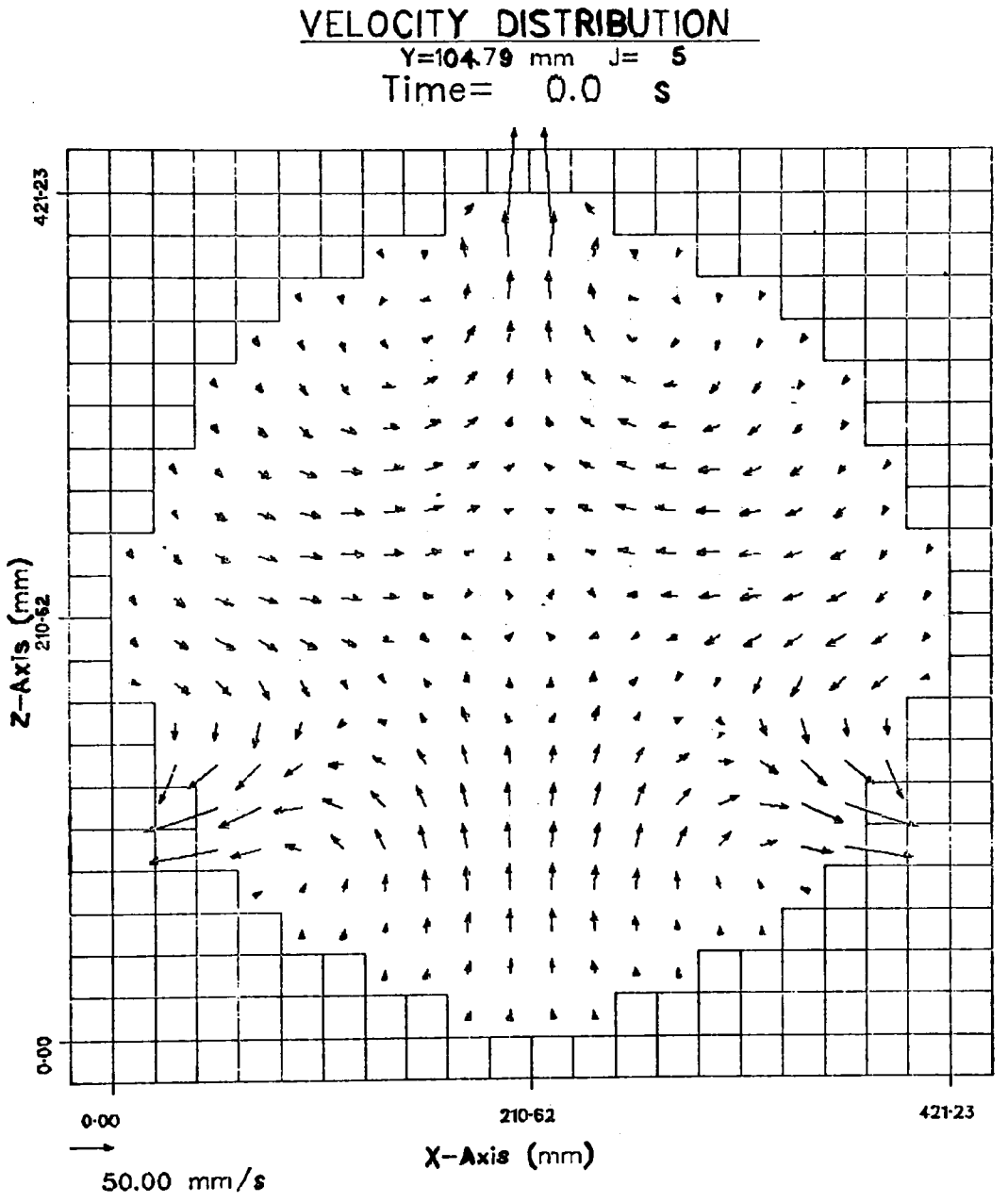

Fig. 6. Velocity Profile Across C-C
ANL Neg No. 116-77-205

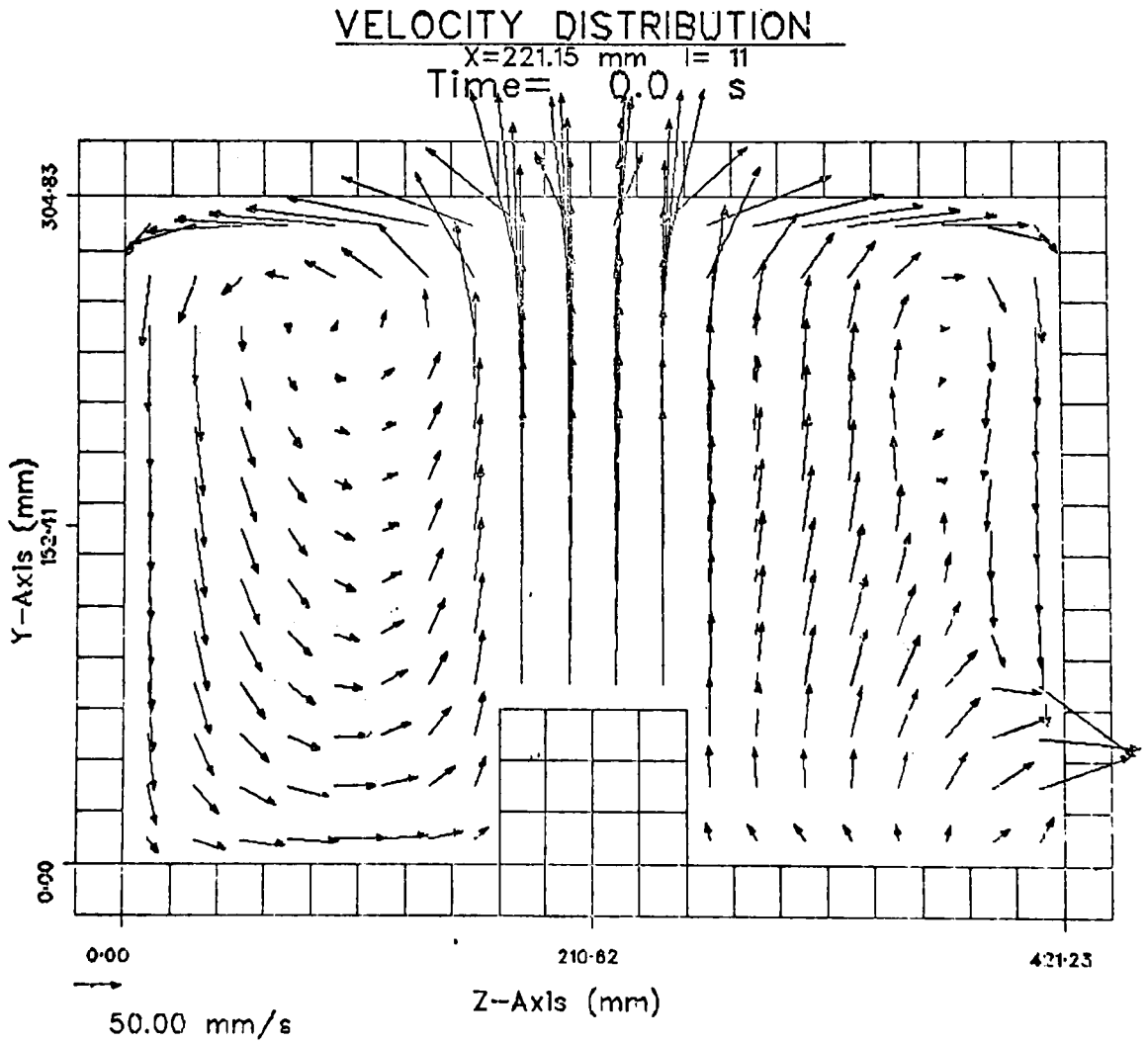

Fig. 7. Velocity Profile Across A-A
ANL Neg. No. 116-77-207

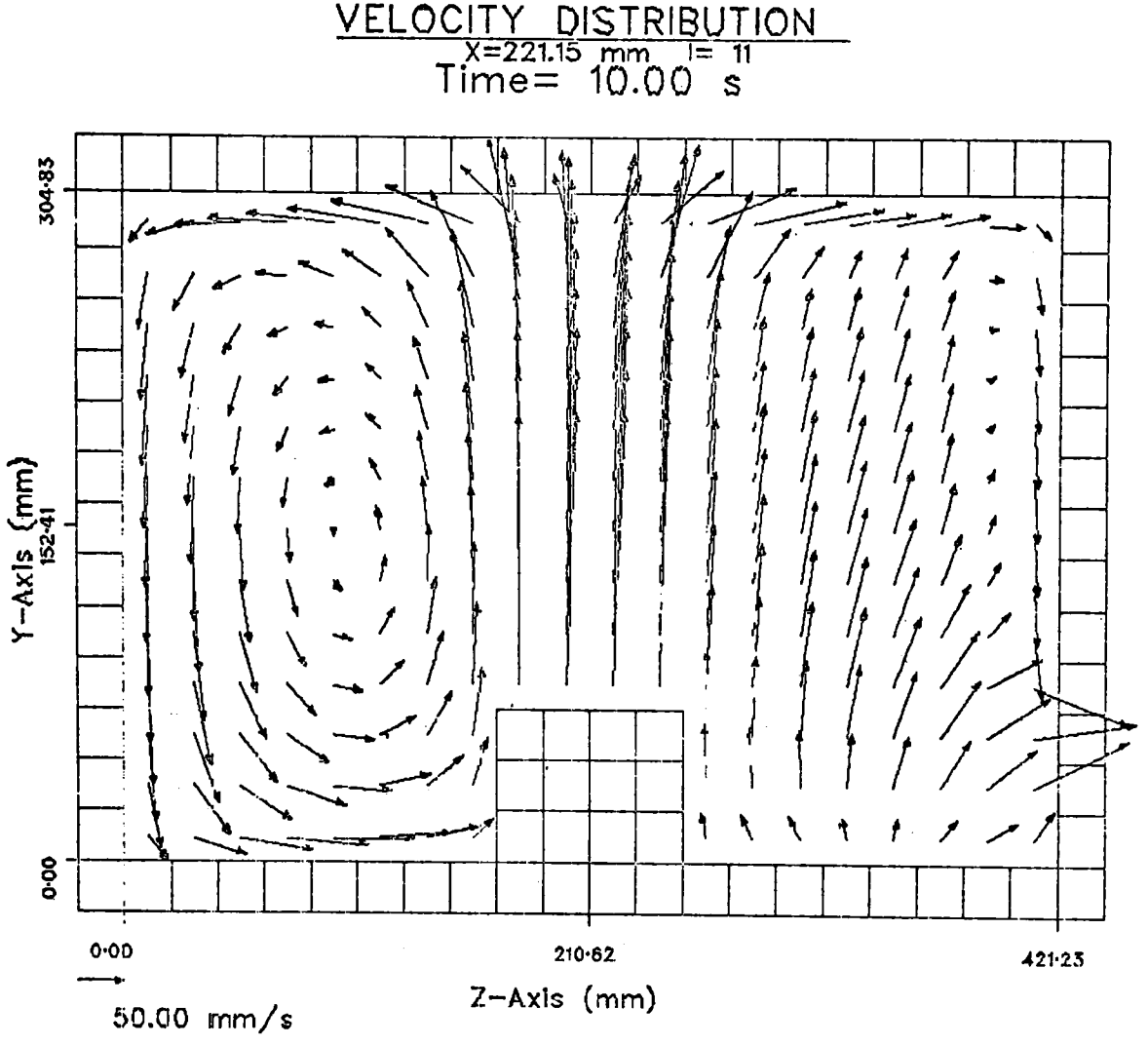

Fig. 8. Velocity Profile Across A-A
ANL Neg. No. 116-77-202

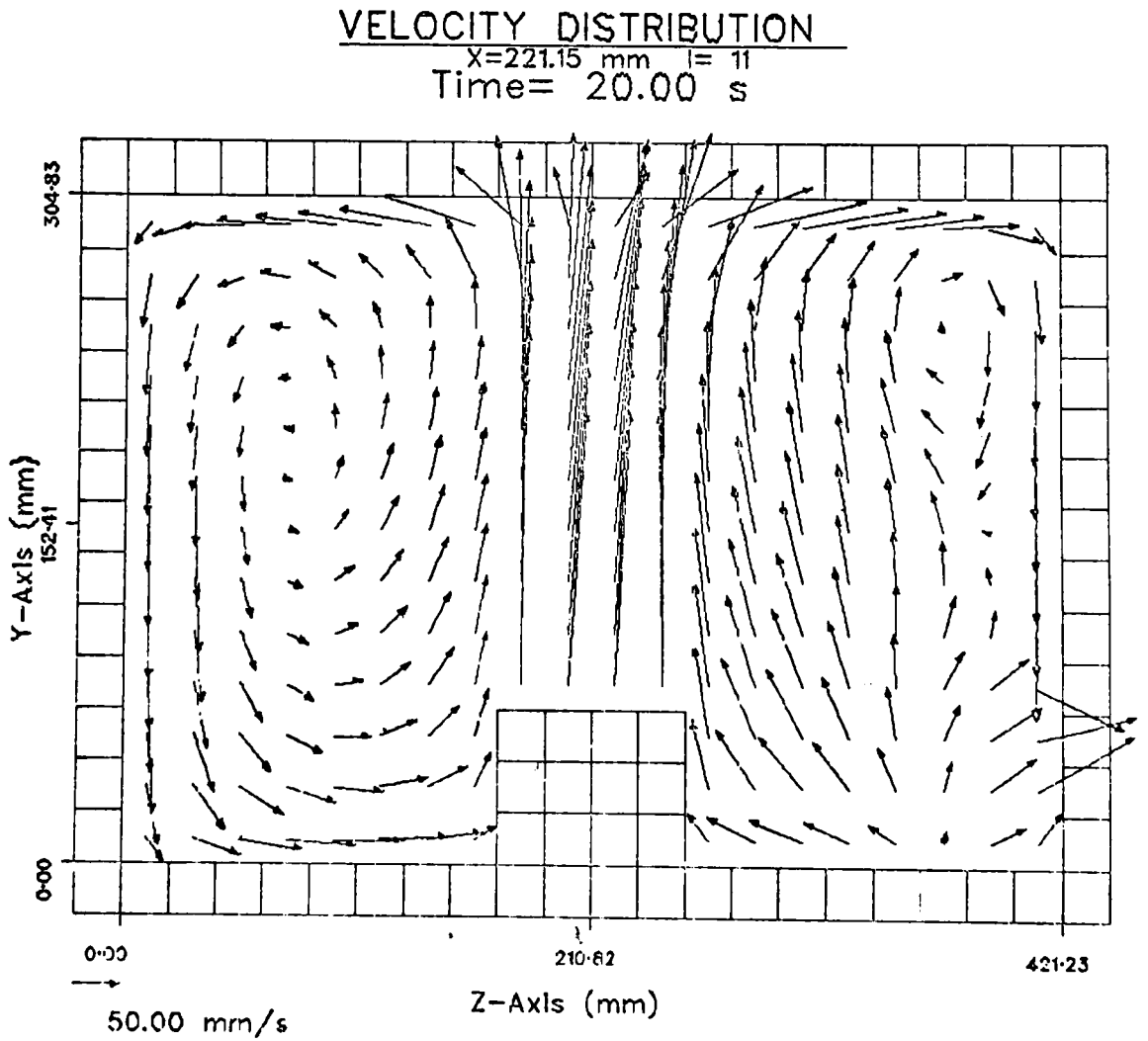

Fig. 9. Velocity Profile Across A-A
ANL Neg. No. 116-77-204

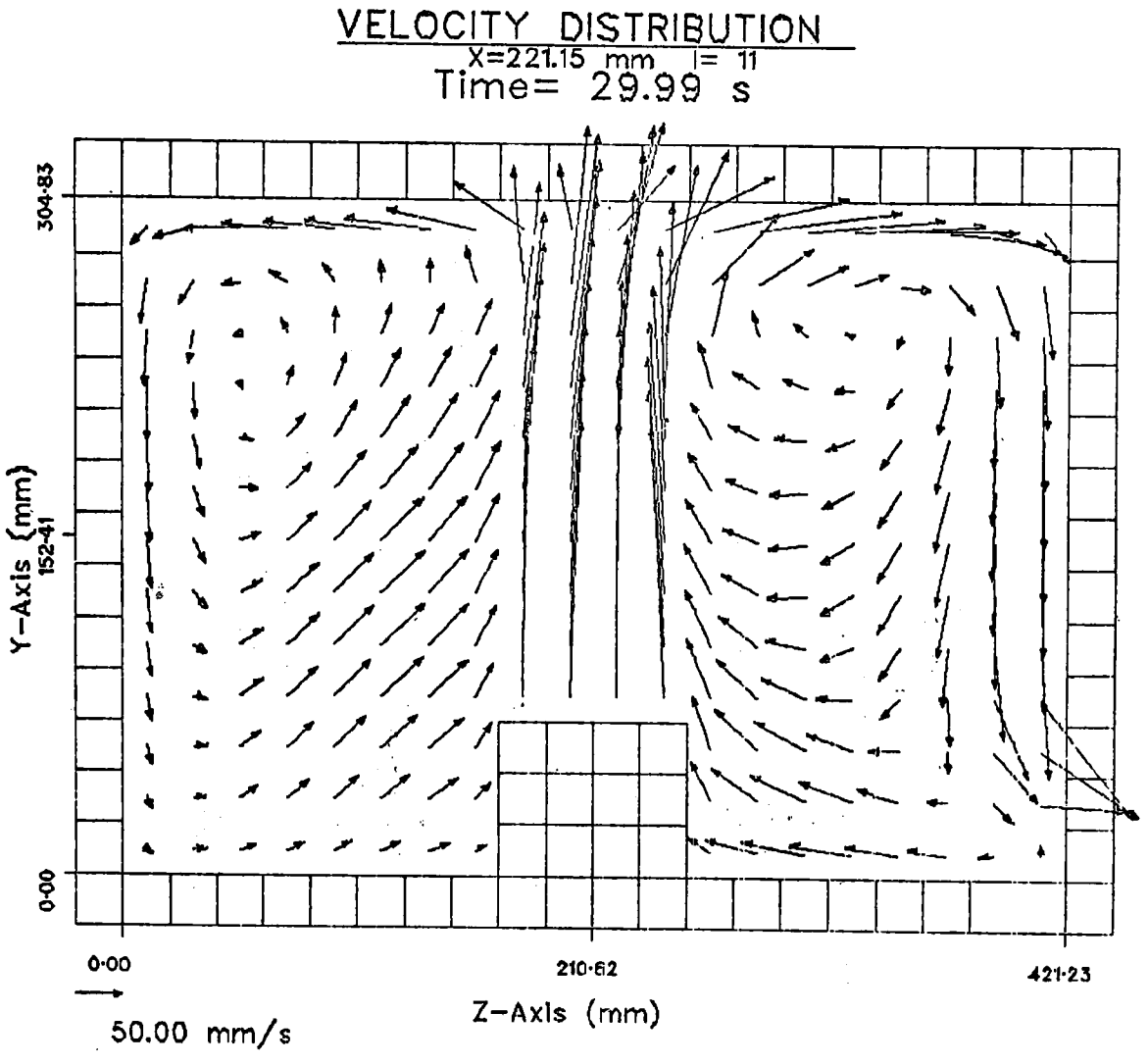

Fig. 10. Velocity Profile Across A-A
ANL Neg. No. 116-77-214

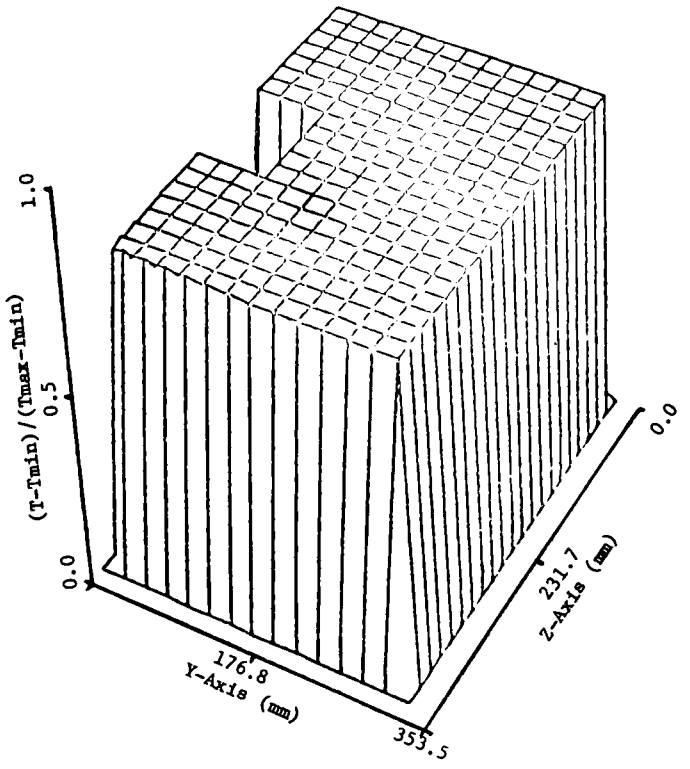

Fig. 11

Temperature Profile
at A-A Time = 0.0 Sec.
ANL Neg. No. 116-77-212

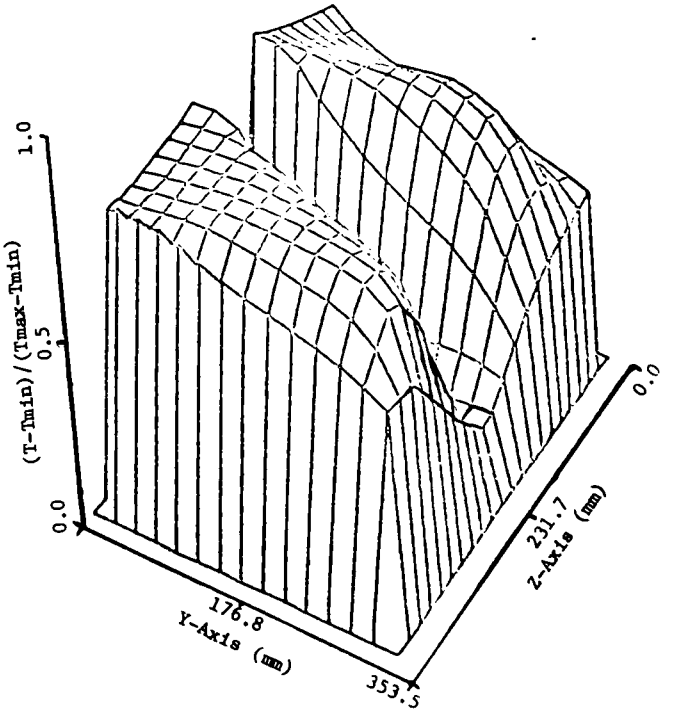

Fig. 12

Temperature Profile at
A-A Time = 10.0 Sec.
ANL Neg. No. 116-77-206

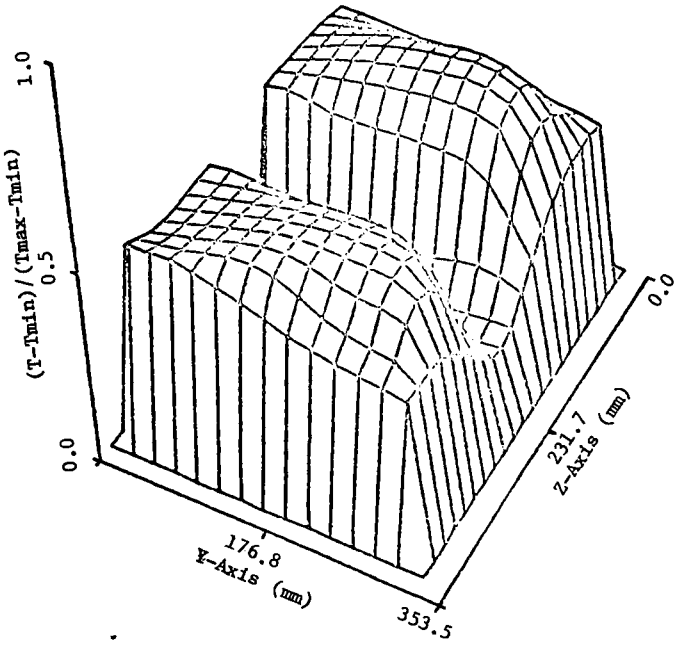

Fig. 13

Temperature Profile at
A-A Time = 20.0 Sec.
ANL Neg. No. 116-77-203

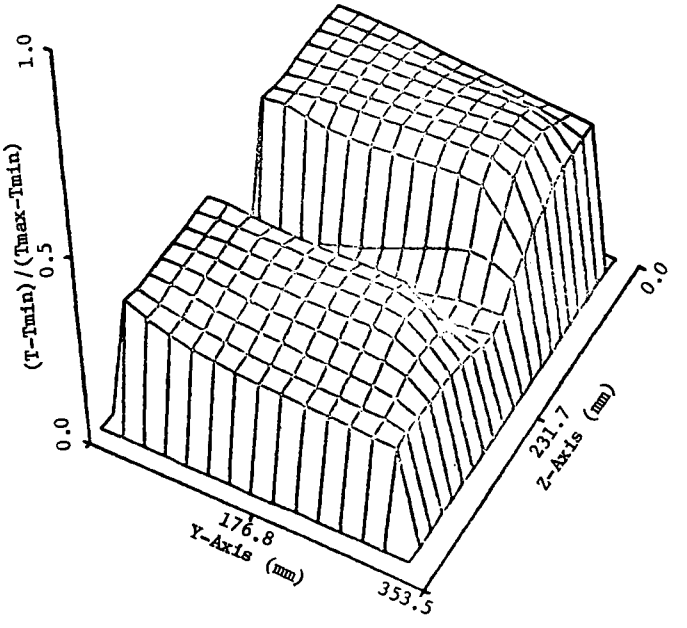

Fig. 14

Temperature Profile at
A-A Time = 30.0 Sec.
ANL Neg. No. 116-77-213

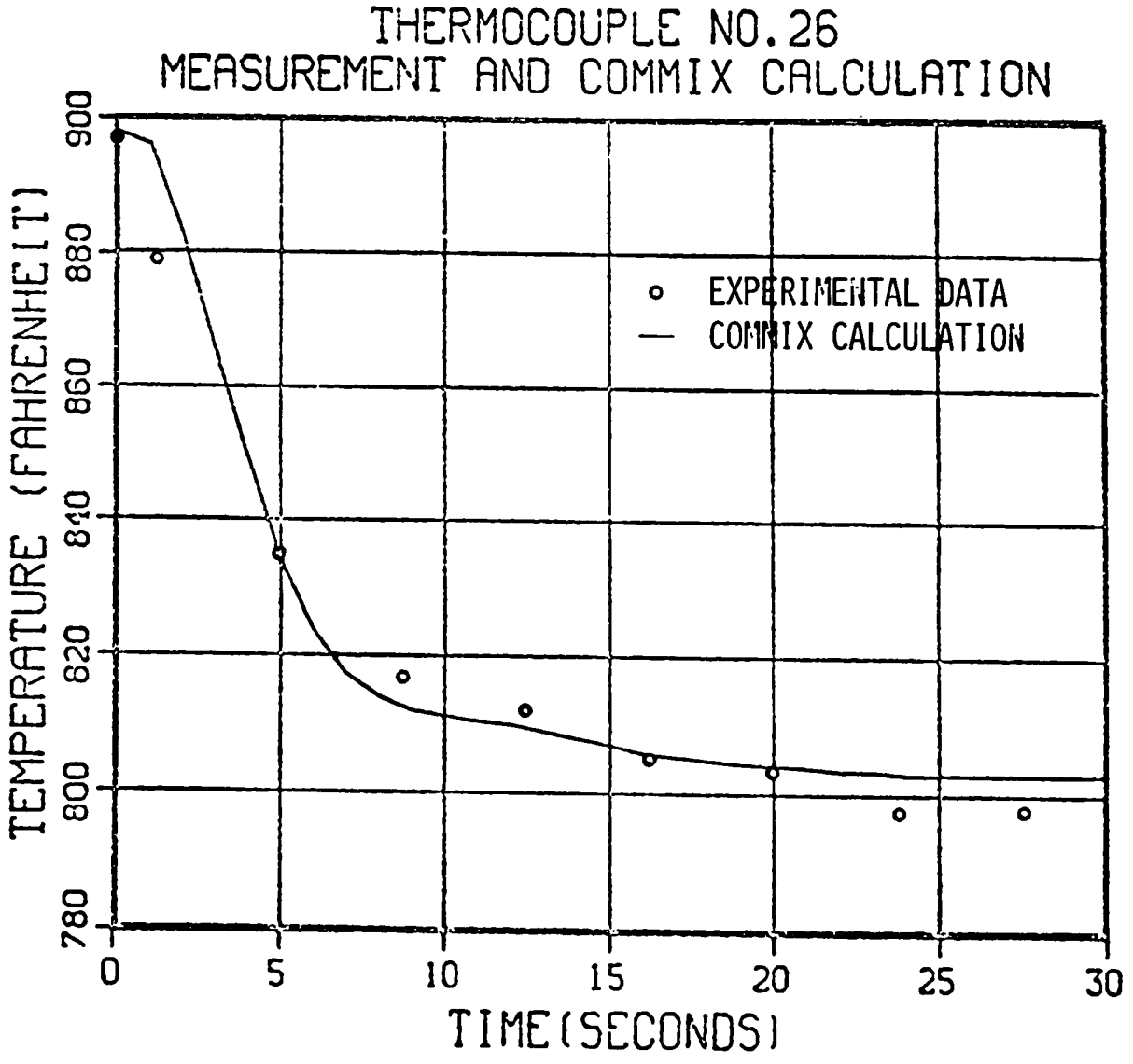

Fig. 15. A Comparison Between Calculated and Measured Temperatures At Outlet Nozzle
ANL Neg. No. 116-77-201

REFERENCES

1. P. M. Wood et al., Private Communication,(October 5, 1976).

2. F. H. Harlow and A. A. Amsden, *Numerical Solution of Almost Incompressible Flow*, Journal of Comp. Physics 3, No. 1, 80-93 (1968).

3. A. D. Grosman, W. M. Pun, A. K. Runchal, D. B. Spalding, and M. Wolfshstein, *Heat and Mass Transfer in Recirculating Flows*, Academic Press (1969).

4. S. V. Patankar and D. B. Spalding, *Numerical Predictions of Three Dimensional Flows*,"Imperial College Mech. Eng. Dept. Report No. HTS/72/25 (1972).

5. B. E. Launder and D. B. Spalding, *Mathematical Models of Turbulence*, Academic Press (1972).

6. C. W. Hirt and J. L. Cook, *Calculating Threee Dimensional Flows Around Structures and Over Rough Terrain*, Journal of Comp. Physics 10, 324-340 (1970).

7. P. J. Roache, *Computational Fluid Mechanics*, Hermosa Publishers (1972).

8. AGARD Lecture Series No. 64, *Advances in Numerical Fluid Mechanics*, presented at the Von Karman Institute (1973).

9. D. B. Spalding, *The Calculation of Convective Heat Transfer in Complex Flow Systems*, Heat Transfer 1974, Vol. IV, proceedings of the 5th International Heat Transfer Conference, Tokyo, Japan.

10. F. H. Harlow and A. A. Amsden, *Numerical Calculation of Multiphase Fluid Flow*, Journal of Comp. Physics 17, 19-52 (1975).

11. F. H. Harlow and A. A. Amsden, *Flow of Interpenetrating Material Phases*, Journal of Comp. Physics 18, 440-464 (1975).

12. J. W. Yang, *An Analysis of Transient Thermal Response in the Outlet Plenum of an LMFBR*, BNL-HUREG-50521 (June, 1976).

13. P. Wood, WARD, Private Communication (1976).

14. J. L. Cook and P. I. Nakayama, *A Computer Program for Calculating Time Dependent Turbulent Fluid Flows with Slight Density Variation*, WARD-0-0106 (July 1975).

15. J. J. Lorenz and R. D. Carlson, *An Investigation of Buoyancy-Induced Flow Stratification in a Cylindrical Plenum*, proceedings of the 1976 Heat Transfer and Fluid Mechnics Institute, University of California, California (June 21-23, 1976).

16. W. T. Sha H. M. Domanus and R. C. Schmitt, *COMTHA--A Three-Dimensional, Transient, Two-Phase Flow with Non-Equilibrium Temperatures and Velocities Thermal-Hydraulic Analysis Computer Program*, ANL-to be published.

17. W. T. Sha and S. L. Soo, *Multidomain Multiphase Fluid Mechanics*, ANL-CT-77-3, to be published 1977.

18. W. T. Sha, H. M. Domanus and A. A. Szweczyk, *Finite Differencing in a 3-D Staggered Mesh Suitable for Irregular Boundary Applications*, ANL-CT-76-56 (December, 1976).